

**Silica diagenesis and its effect on porosity in the
Upper Tor Member, Eldfisk Field, Norway
– a study of 2/7-B-12-A**

Heine Buus Madsen



**Silica diagenesis and its effect on porosity in the
Upper Tor Member, Eldfisk Field, Norway
– a study of 2/7-B-12-A**

Heine Buus Madsen

Table of content

Page

Summary..... 1

1. Introduction 1

2. Geological setting 2

3. Materials and Methods.....2

4. Results3

 4.1 Lithology and mineralogy.....3

 4.2 Petrophysical log characteristics of intervals rich in insoluble residue..... 7

5. Discussion8

 5.1 Source 8

 5.2 Diagenesis..... 8

 5.3 Porosity reduction..... 9

6. Conclusions9

Acknowledgements9

References9

Appendix A i

Silica diagenesis and its effect on porosity in the Upper Tor Member, Eldfisk Field, Norway – a study of 2/7-B-12-A

Madsen, H.B., Geological Survey of Denmark and Greenland, Copenhagen 1350-DK, Denmark

Summary

A core of the Upper Tor Member 10400–10495 ft in 2/7-B-12-A, was investigated to outline the diagenesis of two horizons enriched in insoluble residue at 10420–10431 ft and 10470–10480 ft. The two intervals contain up to 12% insoluble residue, primarily authigenic quartz and kaolinite with subordinate smectite-illite, apatite, crandelite, feldspar, dolomite and pyrite. The source for the quartz, kaolinite and smectite-illite is most likely detrital smectite and feldspar. During burial Mg, Fe and Si were released and substituted by Al in the detrital smectite structure. Dissolution of feldspar contributed with Al, Si and little K to form primarily kaolinite and little smectite-illite. The excess Si precipitated as quartz in close association with kaolinite. The enrichment of insoluble residue in the 10420–10431 ft interval was caused by pressure dissolution, whereas the enrichment in the 10470–10480 ft interval was probably caused by primary enrichment of detrital minerals. Pressure dissolution, precipitation of quartz and formation of kaolinite in pores caused a 10% reduction of the porosity in these intervals, compared to the surrounding, more pure chalk. The insoluble residue enriched intervals are characterized by high RHOB and low NPHI response. Hence the petrophysical logs and crossplots can be used to distinguish intervals with high silicate content and possible porosity reduction.

1. Introduction

The precipitation of diagenetic minerals like quartz and kaolinite affects the permeability and porosity of chalk. The minerals reduce porosity as they precipitate as cement in pores (Maliva and Dickson, 1992; Chaika and Dvorkin, 2000). They can also result in early lithification and then help to preserve porosity during burial to eventually form reservoir rocks (Aase et al., 2001).

Several studies on diagenesis of chalk have been carried out on the North Sea oil fields (Scholle, 1977; Taylor and Lapré, 1987; Maliva et al., 1991; Maliva and Dickson, 1992; Hancock, 1993) but only few have been focused on silica diagenesis (Jakobsen et al., 2000, Fabricius and Borre, 2006; Fabricius et al. 2007). Silica is not a major phase in the chalk but is important in some intervals in the Ekofisk Formation and few intervals in the Tor Formation in the Eldfisk Field. This may indicate that variations are linked to facies and palaeo-oceanography; the silica either representing diagenetically reprecipitated biogenic silica or a high input of detrital minerals and subsequent pressure dissolution (Scholle, 1977; Kennedy, 1987; Fabricius and Borre, 2007).

This report focuses on the diagenesis of quartz- and kaolinite-rich intervals in the deeply buried Upper Tor Member in a core from 2/7-B-12-A, Eldfisk Field, Norwegian North Sea. The main purpose is to understand the diagenetic processes that led to the enrichment and formation of quartz and kaolinite and the following effects on porosity.

2. Geological setting

The Eldfisk Field is located on the Lindesnes ridge in block 2/7 of the Norwegian sector in the Central Graben (Fig. 1a). The Lindesnes Ridge started to form in the early Jurassic by normal faulting, with subsiding fault block creating a basin to the east of the ridge. During the early Cretaceous, inversion of the fault formed the Lindesnes ridge (Michaud, 1987). The Ridge became a structural high from where chalk was eroded and transported to the adjacent basins. The thickness of the chalk is up to 1000 m in the basins and down to 150 m on the crest of the Lindesnes Ridge. During the late Maastrichtian a channel was present in the Eldfisk area just south of the well 2/7-B-12-A, which was drilled in the marginal channel setting (Fig. 1b) (Bramwell et al., 1999, Internal ConocoPhillips report). During the Cretaceous, halokinesis and fault movements caused sporadic reworking in form of slumped debris flows, mud flows and minor turbidites, filling the channel. The halokinesis also formed the structural traps for hydrocarbons.

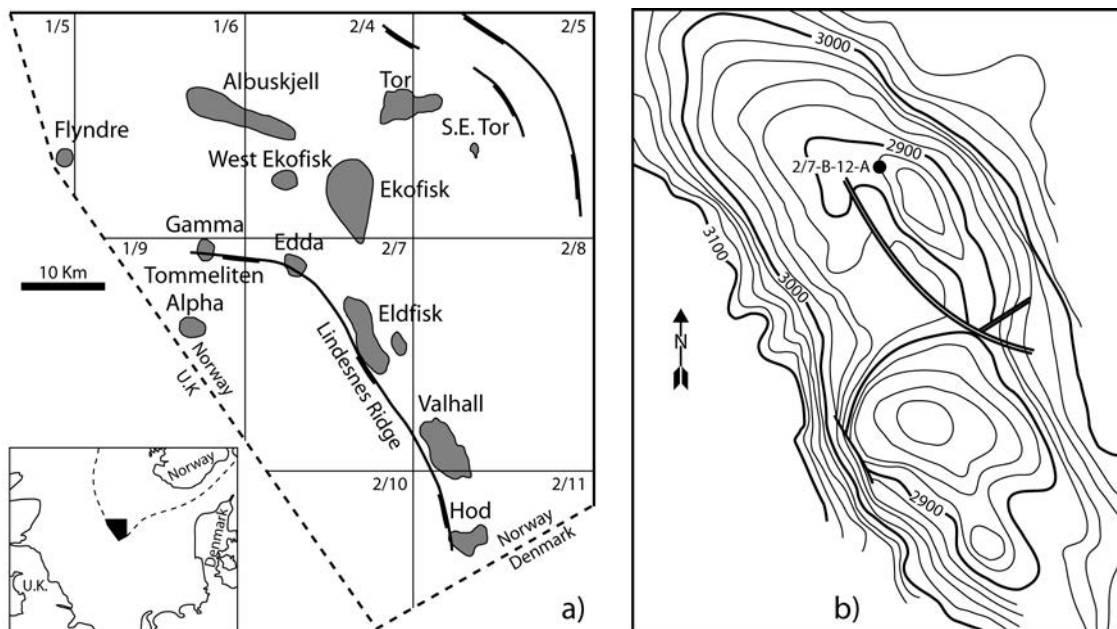


Figure 1. a) Map of the southern Norwegian North Sea with fields and structural elements. b) Top Danian time map of the Eldfisk Field with location of 2/7-B-12-A well. Revised from Michaud (1987).

3. Materials and Methods

The Maastrichtian Tor Formation is subdivided into three units; Lower Tor Member (TC), Middle Tor Member (TB) and Upper Tor Member (TA) in the greater Ekofisk area. 28 samples from the Upper Tor Member in the 10400–10495 ft cored interval in 2/7-B-12-A, have been analysed to investigate the mineralogical composition of the insoluble residue (Appendix A). Samples were crushed in a porcelain mortar until it passed a 2 mm sieve and then cleaned for oil by Soxhlet cleaning in toluene and methanol. When samples were dry, calcite was removed using a buffered acetic acid at pH 4.5. This mild dissolution of the calcite was used to avoid dissolution of non-calcite minerals. X-ray diffraction (XRD) analyses of the insoluble residue were carried out on randomly oriented specimens using a Philips 1050 goniometer with Co-K α radiation (pulse-high

selection and Fe-filter). The amount of quartz in the insoluble residue was determined using 99.99% pure quartz with grain size of 4.5–45 μm as a standard. Other minerals were qualitatively determined by comparing them with standards in the software PW 1877 Automated Powder Diffraction Version 3.6j. SEM analyses were carried out on small samples of chalk and insoluble residue coated with gold in vacuum at 25 kV and 20 mA for 2–3 minutes using a SEM Coating Unit E5000. A PHILIPS XL 40 SEM equipped with a ThermoNoran energy dispersive X-ray detection system (EDX) was used for qualitative chemical analysis and photography. The petrophysical logs NPHI, RHOB and GR were supplied by ConocoPhillips, Norway.

4. Results

4.1 Lithology and mineralogy

In the studied section, 10400–10495 ft in 2/7-B-12-A, the Upper Tor Member consists of a grey chalk with stylolites, argillaceous solution seams, few marly layers and a single bioturbated horizon at 10480 ft (Figs. 2 and 3). The chalk is generally pure, consisting of 96–97% calcite (Fig. 3, Appendix A). The insoluble residue consists primarily of quartz and kaolinite, with subordinate smectite-illite, feldspar, fluor-apatite, crandelite, dolomite, pyrite and fluorite (Fig. 3, Appendix A). However, up to 12% insoluble residue is present in two intervals, 10421–10431 ft and 10470–10480 ft. The 10421–10431 ft interval contains abundant stylolites. Overall the insoluble residue has the same mineralogical composition as the insoluble residue of the pure chalk; with a slightly higher quartz/kaolinite ratio. The 10470–10480 ft interval contains few marl layers, occurs above a thick marl bed and the insoluble residue has a slightly lower quartz/kaolinite ratio than the insoluble residue of the pure chalk.



Figure 2. Core photo of the 10470–10485 ft interval. Note the burrow shaped structures.

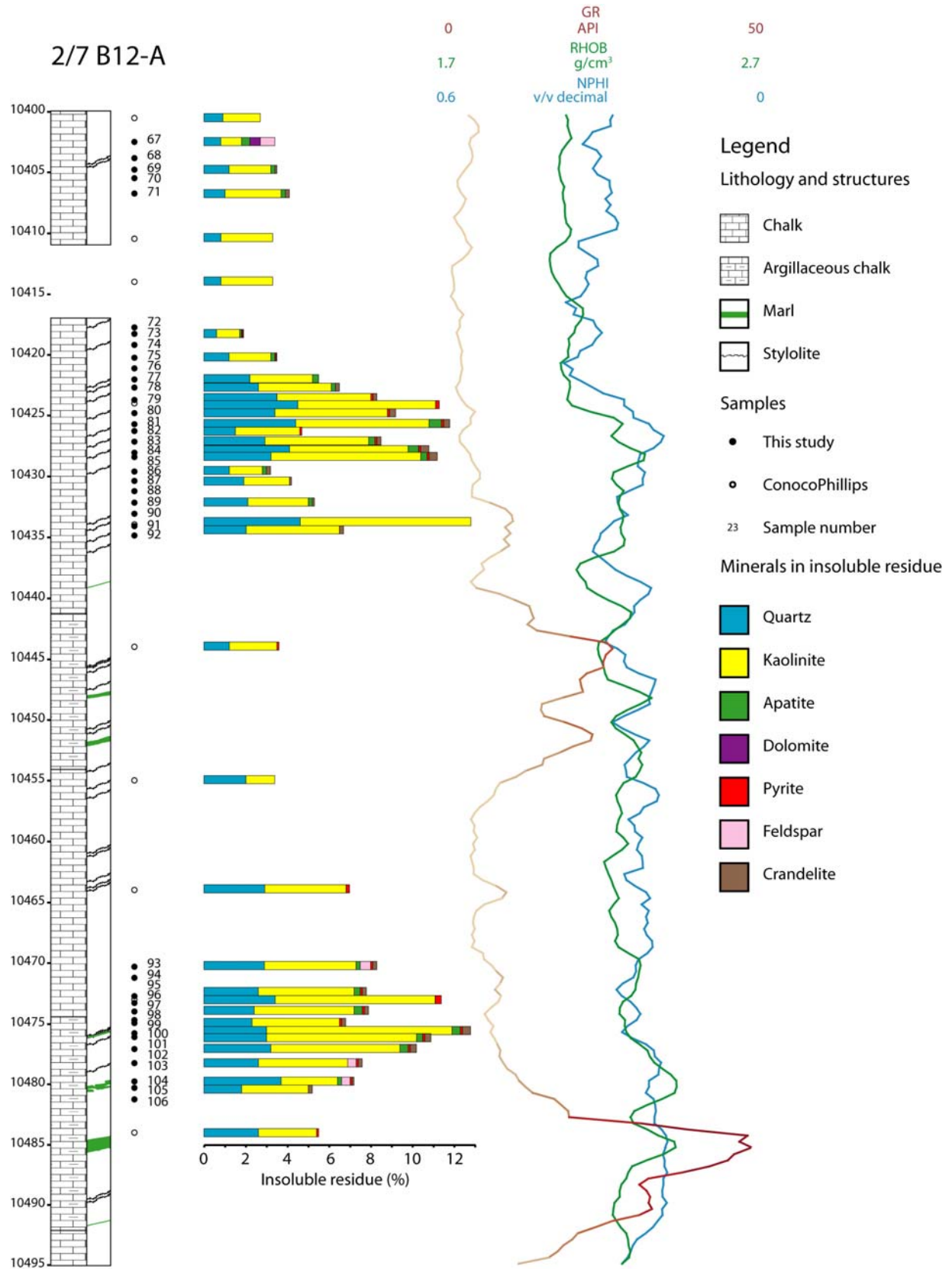


Figure 3. Lithological and petrophysical logs of the Upper Tor Member, 10400–10495 ft interval in the 2/7-B-12-A core. Length of horizontal bars illustrates the amount of insoluble residue and the colours represent the fraction of the different minerals.

Quartz is the most common mineral and occurs as aggregates, euhedral crystals and subhedral crystals. The euhedral crystals are six-sided and single or double terminated by six-faced pyramids and can be up to 10 μm long (Fig. 4a). The aggregates consist of sub-micron-sized quartz crystals and are much smaller, often less than 1 μm (Fig. 4b). Both crystals and aggregates are often associated with kaolinite. Commonly the quartz crystals sit on kaolinite crystals but they are also seen to embed the kaolinite (Fig. 4c). The subhedral quartz crystals, up to 25 μm , embed recrystallized coccolithic fragments and earlier quartz crystals in the 10420–10431 ft interval (Fig. 4d). It shows few well developed crystal faces, commonly with imprints from recrystallized coccolith fragments.

Kaolinite occurs as hexagonal shaped crystals arranged in booklets, commonly around 5 μm in diameter (Fig. 4a, b, c). The kaolinite is present both in voids and in the matrix. It is often associated with quartz aggregates and single quartz crystals (Fig. 4a, b). EDX analyses indicate that the kaolinite primarily consists of Si, Al and O with traces of Ca.

Smectite-illite is present in trace amounts in all samples analysed by XRD (appendix A). It has a flaky and very delicate morphology (Fig. 4e), and chemically it consists of Si, Al, O, with minor amounts of Ca, K and Mg. Feldspar occurs in amounts less than 1% as indicated by the XRD analyses and has not been distinguished in the SEM (Appendix A).

Dolomite has only been distinguished in sample 67 where it comprises 0.5% (Appendix A). The dolomite is rhombohedral, up to 20 μm long (Fig. 4f). The dolomite seems to occur in the matrix where coccolith fragments occasionally have been incorporated in crystal or have left marks on the surface.

Phosphates, fluor-apatite and crandelite ($\text{CaAl}_3(\text{PO}_4)_{1.5}(\text{OH})\cdot 5\text{H}_2\text{O}$) are present in the chalk. Fluor-apatite occurs in most samples in amounts between 0.1–0.6%. The fluor-apatite has not been distinguished in the SEM and is probably present as nano-sized particles which can not be resolved. Crandelite also occur in most samples, comprising 0.1–0.4%. It occurs as aggregates, up to 50 μm , with embedded coccolith fragments (Fig. 4g). EDX analyses indicate a composition of P, Ca, Al, Si, O and occasionally also trace amounts of K and Ti. Pyrite occurs in much of the chalk samples in amounts less than 0.1%. It forms euhedral crystals up to 20 μm with octahedral morphology (Fig. 4h).

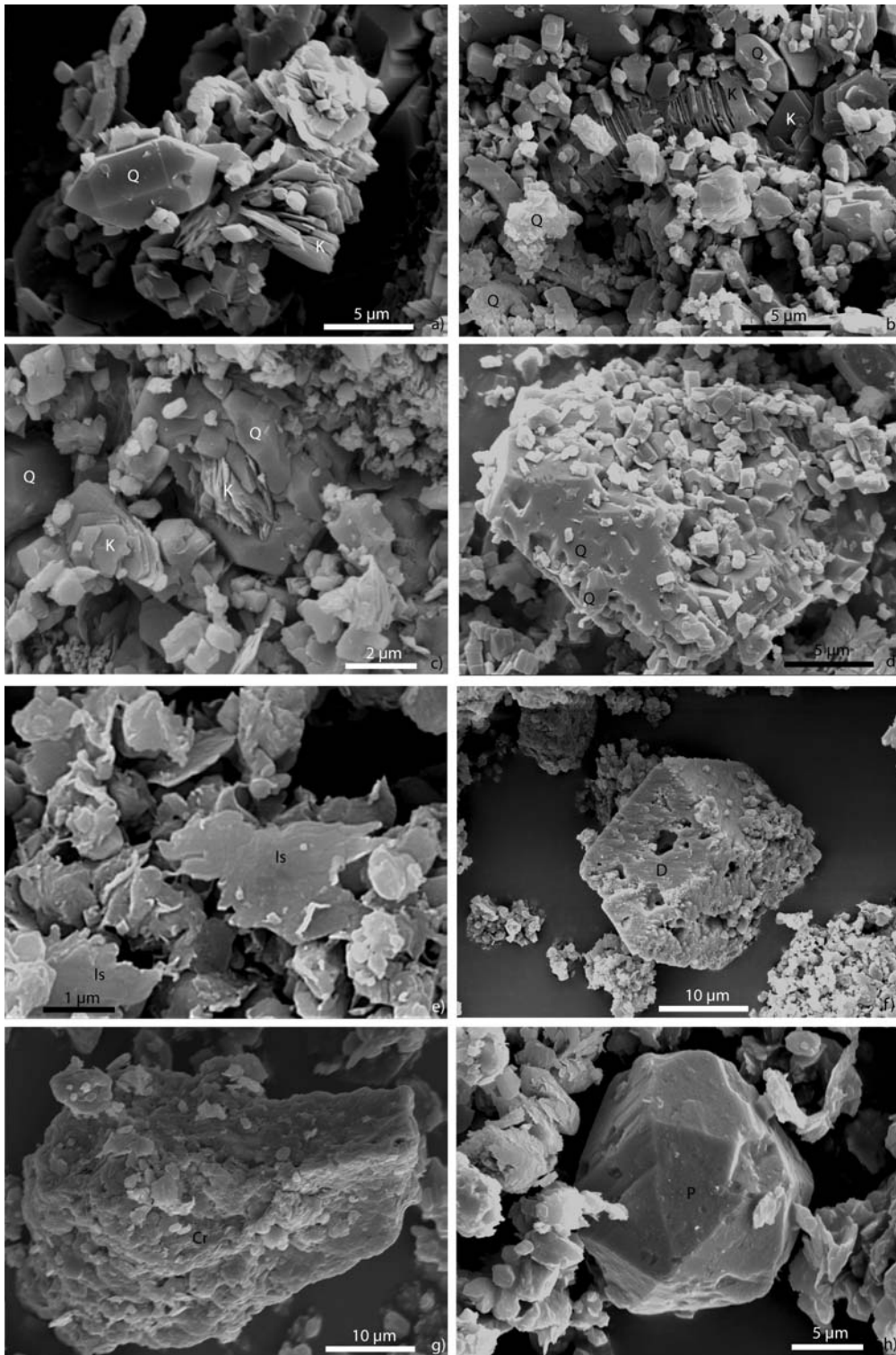


Figure 4. SEM images a) Single quartz crystal (Q) sitting on kaolinite (K). b) Quartz aggregates (lower left corner) consisting of sub-micron sized quartz crystals and booklets of kaolinite in matrix. c) Kaolinite embedded in quartz. d) Quartz cement embedding coccolith fragments and double terminated quartz crystals. e) Flaky smectite-illite (Is) f) Dolomite rhombohedra (D) in insoluble residue, with marks from coccolith fragments. g) Aggregate of crandelite (Cr) with few incorporated coccolith fragments. h) Octahedral pyrite crystal in insoluble residue.

4.2 Petrophysical log characteristics of intervals rich in insoluble residue

The interval 10420–10431 ft contains much more quartz and kaolinite than the surrounding chalk. This interval has low response on the NPHI log and high response on the RHOB log. Peaks in NPHI, RHOB and to some extent in the GR log correlate well with sample 81, 84 and 91, all being rich in quartz, kaolinite and abundant having stylolites (Fig. 3). No obvious peaks in NPHI and RHOB can be correlated to the mineralogy in the kaolinite-dominated 10470–10480 ft interval. This is probably because of the overall lower porosity and higher density in this part of succession (Fig. 3). The GR log to some extent correlates to marls and samples rich in insoluble residue.

A NPHI vs. RHOB cross plot of the studied succession shows that the chalk mainly plots between the sandstone and limestone trends. This is due to the presence of light hydrocarbons (Fig. 5). The intervals rich in insoluble residue have higher density and lower porosity than the surrounding chalk. However, part of the 10420–10431 ft interval has same NPHI and RHOB values as the surrounding chalk, reflecting chalk horizons low in insoluble residue within this interval. The estimated porosity of the chalk is around 35% whereas the silica-rich intervals have porosities around 25% (Fig. 5). The high gamma (dark brown crosses in figure 5) represents marls which also have much lower porosity than the chalk.

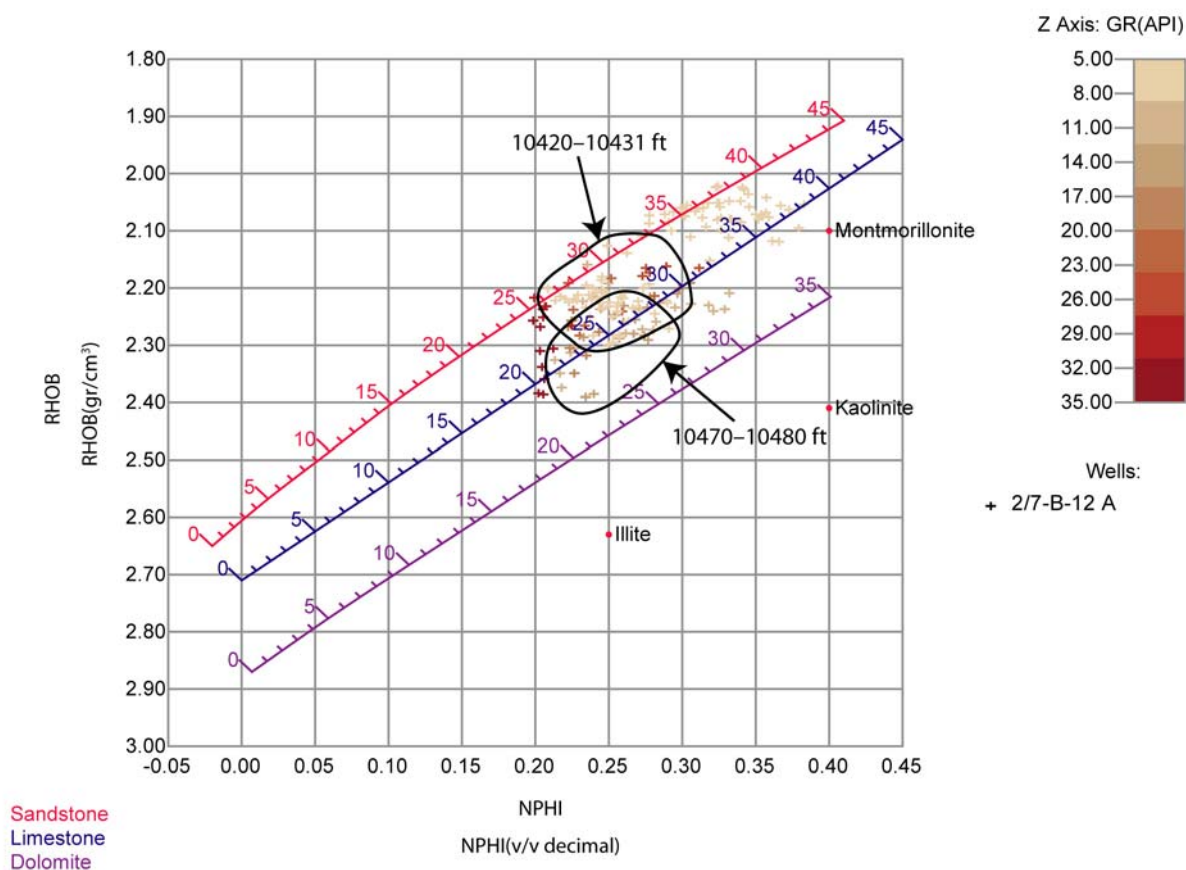


Figure 5. NPHI vs. RHOB cross plot of the 10400–10495 ft interval in 2/7-B-12-A. Trends for sandstone, limestone and dolomite are shown for comparison. The 10420–10431 and 10470–10480 ft intervals are marked with black lines. The pure chalk mostly has high estimated porosity but do also plot within the range of the intervals with high insoluble residue. Darker brown coloured data points indicate high gamma readings from e.g. marl. GR scale bar in the right of the figure.

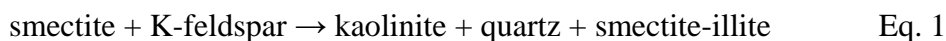
5. Discussion

5.1 Source

The source for the authigenic clay minerals is probably smectite and feldspars which has previously been interpreted to be of terrigenous origin (Kennedy, 1987). The close association between quartz and kaolinite as seen in SEM and XRD indicates that they originate from same mineral reaction, probably from alteration of detrital smectite. A biogenic source for kaolinite is unrealistic as the siliceous skeletons and spicules only contain aluminium in the magnitude of parts per million (Van Bennekom, 1991; DeMaster, 2004). Huge amounts of biogenic silica would be required to form the kaolinite observed and at the same time large quantities of Si would have to disappear out of the system. However, biogenic opal-A from radiolarian or sponge spicule which can be abundant in a marginal channel setting may be an additional source for silica and has also probably contributed to the formation of authigenic quartz, smectite-illite and kaolinite.

5.2 Diagenesis

Some of the quartz is believed to originate from phase transformations of biogenic opal-A to opal-CT and finally to quartz (Williams et al., 1985). But the majority of the quartz is found in close association with kaolinite indicating that quartz also formed from a more complicated mineral reaction during burial. A likely reaction involves the release of silica from silicate minerals as detrital smectite and feldspar. The disappearance of smectite and the formation of illite with depth are well known in the Central Graben, North Sea and other sedimentary basins (Compton, 1991; Abercrombie et al., 1994, Drits et al., 1997). However, since kaolinite is the most abundant clay mineral in the studied interval, a slightly different mineral reaction is suggested where smectite is transformed to primarily authigenic kaolinite and little smectite-illite (Eq. 1). The formation of kaolinite and smectite-illite is probably the result of release of Mg and Fe from the octahedral layer in the smectite (Hower et al., 1976). During this transformation aluminium is conserved in the structure and Si is released (Compton, 1991), which enabled precipitation of quartz near the kaolinite as seen in figure 5c. The released Mg and Fe must have diffused away since no dolomite or other Mg- and Fe-rich minerals have been observed in the chalk. Additional potassium, from K-feldspar or other sources is needed to form smectite-illite (Hoffman and Hower, 1979, Compton, 1991). The fact that kaolinite is the most common authigenic clay mineral indicates that little K-feldspar was available. However, dissolution of plagioclase and K-feldspar has probably contributed with Al, Si and minor K to the formation of kaolinite and smectite-illite, whereas excess Si precipitated as quartz (Eq. 1). The mineral assemblage indicates a potassium poor system explaining the low gamma values recorded in the two intervals.



The presence of abundant stylolites and same mineralogical composition of the insoluble residue in the 10420–10431 ft interval as in the pure chalk, indicate that dissolution of carbonates probably caused the enrichment of insoluble residue in this interval. The co-occurrence of stylolites with samples high in insoluble residue also confirms this. The interval may represent a third of the thickness it had prior to dissolution of carbonates since the content of insoluble residue is three times higher than the surrounding chalk.

The 10470–10480 ft interval does not contain abundant stylolites and dissolution of chalk can not readily explain the enrichment of insoluble minerals. However, marl layers occur in this interval indicating a high primary content of detrital smectite and feldspar thus enabling formation of more quartz and kaolinite during burial (Eq. 1). The marl layer below the 10470–10480 ft interval has a marked peak in the GR log indicating a potassium-rich system, e.g. high primary abundance of K-feldspar, which presumably formed more potassium-rich smectite-illite (Eq. 1).

5.3 Porosity reduction

The precipitation of quartz and formation of kaolinite in pores has reduced the porosity of the chalk especially in the high insoluble residue intervals. This is indicated by the NPHI vs. RHOB cross plot (Fig. 5) which show an estimated porosity of around 25% of the high insoluble residue intervals. This is 10% lower than the surrounding chalk. High porosity of up to 35% in the 10420–10431 ft interval is explained by some intercalations of pure chalk with low insoluble residue. The porosity reduction was probably enhanced by pressure solution in the 10420–10431 ft interval.

6. Conclusions

Two intervals with high content of insoluble residue, up to 12%, were distinguished within the Upper Tor Member in the 2/7-B-12-A core on the Eldfisk Field. The insoluble residue consists of primarily quartz and kaolinite with subordinate smectite-illite. The kaolinite and smectite-illite formed by addition of Al, K and release of Mg, Fe and Si from smectite. Dissolution of feldspar contributed with Al, K and Si. The released Si precipitated as quartz at or near the kaolinite. The intervals represent potassium-poor systems where kaolinite precipitated rather than smectite-illite. The 10420–10431 ft interval was probably enriched in insoluble residue by pressure dissolution, as indicated by the presence of abundant stylolites. The high content of insoluble residue in the 10470–10480 ft was probably caused by high content of detrital minerals poor in K. The kaolinite and quartz caused a reduction of the porosity in the high insoluble residue intervals with around 10%, compared to the surrounding pure chalk. The NPHI and RHOB logs can be used to identify intervals rich in quartz and kaolinite, whereas the GR log is not suitable, probably because the studied intervals were potassium poor.

Acknowledgement

ConocoPhillips Norway is thanked for financial support, providing core material and geophysical logs. Finn Christian Jakobsen, Geological Survey of Denmark and Greenland, is thanked for discussions and Per Ekelund Andersen, Geological Survey of Denmark and Greenland, kindly helped with introduction to Openworks.

References

Aase, N.E.; Bjorkum, P.A. and Nadeau, P.H. (2001). The effect of grain-coating microquartz on preservation of reservoir porosity, *The American Association of Petroleum Geologists Bulletin* 80: 1654–1673.

- Abercrombie, H.J.; Hutcheon, I.E.; Bloch, J.D. and Decaritat, P. (1994). Silica activity and the smectite-illite reaction, *Geology* 22(6): 539–542.
- Bramwell, N.P.; Caillet, G.; Meciani, L.; Judge, N.; Green, N. and Adam, P. (1999). Chalk exploration, the search for a subtle trap, *in* Fleet, A.J. and Boldy, S.A.R., *Petroleum Geology of Northwestern Europe*, London, England, The Geological Society, London: 911–937.
- Chaika, C. and Dvorkin, J. (2000). Porosity reduction during diagenesis of diatomaceous rocks. *The American Association of Petroleum Geologists Bulletin* 84(8): 1173–1184.
- Compton, J.S. (1991). Origin and diagenesis of clay minerals in the Monterey Formation, Santa Maria Basin area, California. *Clays and Clay Minerals* 39(5): 449–466.
- Demaster, D.J., 2004, The diagenesis of biogenic silica: chemical transformations occurring in the water column, seabed, and crust, *in* Holland, H.D. and, Turekian, K.K., eds., *Treatise on geochemistry*, Amsterdam, Elsevier Ltd, p. 87–98.
- Drits, V.A.; Sakharov; B.A.; Lindgreen, H. and Salyn, A. (1997). Sequential structure transformation of illite-smectite-vermiculite during diagenesis of Upper Jurassic shales from the North Sea and Denmark. *Clay Minerals* 32: 351–371.
- Fabricius, I.L. and Borre, M.K. (2007). Stylolites, porosity, depositional texture, and silicates in chalk facies sediments. Ontong Java Plateau - Gorm and Tyra fields North Sea. *Sedimentology* 54: 183–205.
- Fabricius, I.L., Røgen, B. and Gommesen, L. (2007). How depositional texture and diagenesis control petrophysical and elastic properties of samples from five North Sea chalk fields. *Petroleum Geoscience* 13: 81–95.
- Hancock, J.M. (1993). The formation and diagenesis of chalk, *in* Downing, R.A.; Price, M. and Jones, G.P., *The hydrology of the chalk of the north-west Europe*. Oxford: 14–34.
- Hoffman, J. and Hower, J. (1979). Clay mineral assemblages as low grade metamorphic geothermometers: Application to the thrust faulted disturbed belt of Montana, U.S.A., *in* Scholle, P.A. and Schluger, P.R., *Aspects of diagenesis.*, SEPM Special Publications. 26: 55–79.
- Hower, J.; Eslinger, E.V.; Hower, M. and Perry, E.A. (1976). The mechanism of burial metamorphism of argillaceous sediments: 1. mineralogical and chemical evidence. *Geological Society of America Bulletin* 87: 725–737.
- Jakobsen, F.; Lindgreen, H. and Springer, N. (2000). Precipitation and flocculation of spherical nano-silica in North Sea chalk. *Clay Minerals* 35: 175–184.
- Kennedy, W.J. (1987). Sedimentology of Late Cretaceous-Paleocene chalk reservoirs, North Sea Central Graben, *in* Brooks, J. and Glennie, K. *Petroleum Geology of the North West Europe*. London, Graham and Trotman: 469–481.

- Maliva, R.G. and Dickson, J.A.D. (1992). Microfacies and diagenetic controls of porosity in Cretaceous/Tertiary chalks, Eldfisk, norwegian North Sea. *The American Association of Petroleum Geologists Bulletin* 76(11): 1825-1838.
- Michaud, F. (1987). Eldfisk, *in* Spencer, A.M.; et al. (eds) *Geology of the Norwegian oil and gas fields*, Graham and Trotman: 89–105.
- Scholle, P.A. (1977). Chalk Diagenesis and Its Relation to Petroleum Exploration. *The American Association of Petroleum Geologists Bulletin* 61(7): 982–1009.
- Taylor, S.R. and Lapré, J.F. (1986). North Sea chalk diagenesis: its effect on reservoir location and properties, *in* Brooks, J. and Glennie K.W. *3rd Conference on petroleum geology of North West Europe*, London, England, Graham and Trotman Ltd. 483-495
- Van Bennekom, A.J.; Buma, A.G.J. and Nolting, R.F. (1991). Dissolved aluminum in the Weddell-Scotia confluence and effect of Al on the dissolution kinetics of biogenic silica. *Marine Chemistry* 35: 423–434.
- Williams, L.A.; Parks, G.A. Crerar, David A. (1985). Silica Diagenesis, I. Solubility Controls. *Journal of Sedimentary Petrology* 55(3): 301–311.

Appendix A

2/7-B-12-A Plug	Core	Depth		Zone	Lithology	Bulk (gr.)	ISR (gr.)	ISR (%)	Minerals in chalk (%)									
		(ft)	(inc)						Calcite	Quartz	Kaolinite	Apatite	Crandelite	Dolomite	Feldspar	Pyrite	Flourite	smectite-Illite
67	3	10402	0	TA	Chalk	34.8	1.2	3.4	96.6	0.8	1.0	0.4	0.0	0.5	0.7	0.0	0.0	SI
68	3	10403	9	TA	Chalk													
69	3	10404	9	TA	Chalk	32.4	1.2	3.6	96.4	1.2	2.0	0.2	0.1	0.0	0.0	0.0	0.0	SI
70	3	10405	6	TA	Chalk													
71	3	10406	7	TA	Chalk	29.6	1.2	4.1	95.9	1.0	2.7	0.2	0.2	0.0	0.0	0.0	0.0	SI
72	4	10417	8	TA	Chalk													
73	4	10418	5	TA	Chalk	38.9	0.8	2.0	98.0	0.6	1.1	0.1	0.0	0.0	0.0	0.0	0.1	SI
74	4	10419	3	TA	Chalk													
75	4	10420	4	TA	Chalk	37.0	1.3	3.4	96.6	1.2	2.0	0.2	0.0	0.0	0.0	0.0	0.1	SI
76	4	10421	1	TA	Chalk													
77	4	10421	11	TA	Chalk	37.8	2.1	5.5	94.5	2.2	3.0	0.3	0.0	0.0	0.0	0.0	0.0	SI
78	4	10422	8	TA	Chalk	28.1	1.8	6.5	93.5	2.6	3.5	0.2	0.2	0.0	0.0	0.0	0.0	SI
79	4	10423	6	TA	Chalk	35.3	2.9	8.3	91.7	3.5	4.5	0.0	0.2	0.0	0.0	0.1	0.0	SI
80	4	10424	9	TA	Chalk	33.1	3.0	9.2	90.8	3.4	5.4	0.0	0.3	0.0	0.0	0.1	0.0	SI
81	4	10425	9	TA	Chalk	39.4	4.6	11.8	88.2	4.4	6.4	0.6	0.3	0.0	0.0	0.1	0.0	SI
82	4	10426	6	TA	Chalk	34.0	1.6	4.8	95.2	1.5	3.1	0.0	0.1	0.0	0.0	0.0	0.0	SI
83	4	10426	10	TA	Chalk	34.8	3.0	8.5	91.5	2.9	5.0	0.3	0.3	0.0	0.0	0.1	0.0	SI
84	4	10427	8	TA	Chalk	32.4	3.4	10.4	89.6	4.1	5.7	0.2	0.4	0.0	0.0	0.1	0.0	
85	4	10428	10	TA	Chalk	34.6	3.9	11.2	88.8	3.2	7.2	0.3	0.4	0.0	0.0	0.1	0.0	SI
86	4	10429	9	TA	Chalk	26.5	0.8	3.0	97.0	1.2	1.6	0.1	0.1	0.0	0.0	0.0	0.0	SI
87	4	10430	6	TA	Chalk	34.9	1.5	4.2	95.8	1.9	2.2	0.0	0.1	0.0	0.0	0.0	0.0	SI
88	4	10431	5	TA	Chalk													
89	4	10432	3	TA	Chalk	24.9	1.3	5.3	94.7	2.2	2.8	0.2	0.1	0.0	0.0	0.0	0.0	SI
90	4	10433	3	TA	Chalk													
91	4	10434	2	TA	Chalk	36.3	2.5	6.8	93.2	2.0	4.5	0.0	0.2	0.0	0.0	0.0	0.0	SI
92	4	10434	11	TA	Chalk													
93	5	10470	5	TA	Chalk	41.9	3.4	8.2	91.8	2.9	4.4	0.2	0.2	0.0	0.5	0.1	0.0	SI
94	5	10471	4	TA	Chalk													
95	5	10472	10	TA	Chalk	45.0	3.5	7.8	92.2	2.6	4.6	0.3	0.2	0.0	0.0	0.1	0.0	SI
96	5	10473	3	TA	Chalk													
97	5	10473	11	TA	Chalk	43.6	3.4	7.9	92.1	2.4	4.8	0.4	0.2	0.0	0.0	0.1	0.0	SI
98	5	10474	9	TA	Chalk													
99	5	10475	0	TA	Chalk	38.1	2.6	6.8	93.2	2.3	4.2	0.0	0.2	0.0	0.0	0.1	0.0	SI
100	5	10475	10	TA	Chalk	45.4	5.8	12.8	87.2	3.0	8.9	0.4	0.4	0.0	0.0	0.1	0.0	SI
101	5	10476	2	TA	Chalk	38.6	4.2	10.8	89.2	3.0	7.2	0.3	0.3	0.0	0.0	0.1	0.0	SI
102	5	10477	2	TA	Chalk	44.3	4.5	10.1	89.9	3.2	6.2	0.4	0.3	0.0	0.0	0.1	0.0	SI
103	5	10478	3	TA	Chalk	37.5	2.9	7.6	92.4	2.6	4.3	0.0	0.2	0.0	0.4	0.1	0.0	SI
104	5	10479	8	TA	Chalk	38.3	2.8	7.2	92.8	3.7	2.7	0.2	0.1	0.0	0.4	0.1	0.0	SI
105	5	10480	5	TA	Chalk	39.7	2.1	5.3	94.7	1.8	3.2	0.0	0.2	0.0	0.0	0.0	0.0	SI
106	5	10481	4	TA	Chalk													

Also present but not quantified

ISR: insoluble residue

S:Smectite

SI: smectite-Illite